Theoretical study of wave propagation along the coaxial waveguide filled with moving magnetized plasma*

Zhang Ya-Xin(张雅鑫)[a)†], Jia Jia(贾 佳)[a)b)],
Liu Sheng-Gang(刘盛纲)[a)], and Yan Yang(鄢 扬)[a)]

[a)] *Research Institute of High Energy Electronics, University of Electronics Science and Technology of China, Chengdu* 610054, *China*
[b)] *Chengdu University of Information Technology, Chengdu* 610225, *China*

(Received 17 February 2010; revised manuscript received 29 March 2010)

This paper presents detailed theoretical study on the theory of wave propagation along the coaxial waveguide filled with moving magnetized plasma (CWMMP). Making use of the Lorentz transformation and the constitutive transformation, Maxwell's equations lead to the coupled non-homogeneous differential equations which govern the wave propagation in CWMMP, and then analytical solutions have been obtained. The discussion about the eigenvalues of the waves and detailed studies on the fields are carried out. It finds that the fields of the CWMMP are composed of two parts with different eigenvalues. Numerical calculations show that because of Doppler shift effect, the eigenvalues of the modes in such a case is quite different from those of the CWMMP. And a detailed discussion on the dispersion characteristic of CWMMP is presented.

Keywords: moving magnetized plasma, dispersion characteristic

PACC: 5275, 5240d, 1150

1. Introduction

The microwave electronics devices have great achievements in recent years.[1−3] However, further enhancement of output power and efficiency of this device faces some fundamental limits. One of the most important limits is the space charge effect due to mutual repulsion of the electrons that limits the maximum current density due to the beam "blow-up" instability. And the space charge causes the potential at the centre of the electron beam to be lower than that on the outer surface of the beam. This effect may thus also cause defocusing the beam, degrading the beam quality. These and other effects of space charge seriously perturb beam–wave interactions and degrade the performance and behaviour of microwave devices.

The most promising approach for increasing the beam current density is introducing a background plasma fill.[4−7] It has already been shown that plasma fill can dramatically enhance the output power and efficiency of some microwave devices, such as the plasma Cherenkov radiation devices. So a number of papers addressing various aspects of this plasma-filled device have been published and many papers are concerned with the theory of electromagnetic wave-beam interaction in plasma-filled microwave devices and two-beam instability.[8−12] However, the theory is very complex. Recently, there has been an effective solution to solve the problem, which supposes that the electron beam with confined magnetic field equals moving magnetized plasma (MMP) in the waveguide,[12] and because of the electrostatic effect the head part of the electron beam can exclude the electrons from the plasma to generate an ion channel, in this case the background plasma can be considered as two parts, one is steady plasma and another is static ion channel. In this way the beam can be simplified as a group of slow and fast waves and the problem of wave-beam interaction can be simplified to the instability of the slow waves of MMP between the background plasma. Thus the most important problem of this solution is analysing the dispersion characteristics of such equivalent MMP in

*Project supported by the National Natural Science Foundation of China (Grant No. 60877058).
†Corresponding author. E-mail: iamaxin@tom.com
© 2010 Chinese Physical Society and IOP Publishing Ltd

the waveguide. So dealing with the dispersion characteristics of devices filled with equivalent MMP is very important for beam-wave interaction immersed in a finite magnetic field and the study of slow wave theory. Nevertheless, there are only a few papers dealing with the problem of moving plasma.[11−17] In Refs. [12] and [17], the study on the dispersion characteristics of MMP in the circular waveguide has been studied and some significant results have been presented.

Based on the theory of Refs. [12] and [17], detailed theoretical investigation and computer calculations on the dispersion characteristic of coaxial waveguide filled with equivalent moving magnetized plasma (CWMMP) are studied in this paper. More detailed study about the eigenvalues which determine the dispersion characteristics has been presented and the comparison between the characteristics of CWMMP and MMP in the circular waveguide[17] is discussed.

2. Basic equations

In this section, we are going to investigate the dispersion characteristics of CWMMP, for doing this, we need to use two coordinates, one is MMP coordinate, the moving frame, and another is stationary coordinate, the Lab frame. In our theoretical model, we assume that the magnetized plasma is moving along z axis with velocity v_0 and there is a finite homogeneous magnetic field B_z along the z axis as shown below. And we consider that the process of MMP in the waveguide is instantaneous (< 1 ms) and steady, so the effect between plasma and wall of waveguide can be ignored.

In the moving frame, the dielectric tensor of the MMP is as follows:

$$\boldsymbol{\varepsilon}' = \varepsilon_0 \begin{bmatrix} \varepsilon_1' & -\mathrm{i}\varepsilon_2' & 0 \\ \mathrm{i}\varepsilon_2' & \varepsilon_1' & 0 \\ 0 & 0 & \varepsilon_3' \end{bmatrix}. \tag{1}$$

The superscript "$'$" represents the physical quantities in the moving frame. Where

$$\varepsilon_1' = -\frac{\left(\omega_{\mathrm{p}}'^2\right)}{\left(\omega'^2 - \omega_{\mathrm{c}}'^2\right)} + 1, \quad \varepsilon_2' = \frac{\omega_{\mathrm{p}}'^2 \omega'_{\mathrm{c}}}{\omega'\left(\omega'^2 - \omega_c'^2\right)},$$
$$\varepsilon_3' = 1 - \frac{\omega_{\mathrm{p}}'^2}{\omega'^2}, \quad \omega_p'^2 = \frac{e^2 n_0}{m_0 \varepsilon_0}\gamma = \omega_p^2 \gamma,$$
$$\omega_{\mathrm{c}}^2 = \omega_{\mathrm{c}}^2 \gamma^2, \quad \omega'^2 = \omega^2 \gamma^2,$$

where ω_{p} is the plasma frequency, ω_{c} is the electron cyclotron frequency, n_0 is the plasma density, γ is the Fitzgerald–Lorentz contraction factor $\gamma = 1/\sqrt{1-\beta^2}$, and β is the relativistic speed ratio v_0/c_0. Making use of the Lorentz transformation and constitutive transformation, we can transform the tensor and fields from the moving frame into the stationary frame. Then we obtain the transformed fields in the Lab frame as[12,17]

$$\boldsymbol{D} = \boldsymbol{\varepsilon} \cdot \boldsymbol{E} + \boldsymbol{\xi} \cdot \boldsymbol{H}_T, \quad \boldsymbol{B} = \boldsymbol{\mu} \cdot \boldsymbol{H} - \boldsymbol{\xi} \cdot \boldsymbol{E}_{\mathrm{T}}, \tag{2}$$

$$\boldsymbol{\varepsilon} = \varepsilon_0 \begin{bmatrix} \varepsilon_1^* & -\mathrm{i}\varepsilon_2^* & 0 \\ \mathrm{i}\varepsilon_2^* & \varepsilon_1^* & 0 \\ 0 & 0 & \varepsilon_3^* \end{bmatrix}, \quad \boldsymbol{\mu} = \mu_0 \begin{bmatrix} \mu_1^* & -\mathrm{i}\mu_2^* & 0 \\ \mathrm{i}\mu_2^* & \mu_1^* & 0 \\ 0 & 0 & \mu_3^* \end{bmatrix}, \quad \boldsymbol{\xi} = \frac{v_0}{c_0^2} \begin{bmatrix} -\mathrm{i}\xi_g^* & -\xi^* & 0 \\ \xi^* & -\mathrm{i}\xi_g^* & 0 \\ 0 & 0 & 0 \end{bmatrix}, \tag{3}$$

where

$$\varepsilon_1^* = \frac{1-\beta^2}{\left[\left(1-\varepsilon_1'\beta^2\right)^2 - \left(\varepsilon_2'\beta^2\right)^2\right]}\left[\left(1-\varepsilon_1'\beta^2\right)\varepsilon_1' + \left(\varepsilon_2'\beta\right)^2\right], \quad \varepsilon_2^* = \frac{\left(1-\beta^2\right)}{\left[\left(1-\varepsilon_1'\beta^2\right)^2 - \left(\varepsilon_2'\beta^2\right)^2\right]}\varepsilon_2',$$
$$\varepsilon_3^* = \varepsilon_3', \quad \mu_1^* = \frac{1-\beta^2}{\left[\left(1-\varepsilon_1'\beta^2\right)^2 - \left(\varepsilon_2'\beta^2\right)^2\right]}\left(1-\varepsilon_1'\beta^2\right), \quad \mu_2^* = \frac{\left(1-\beta^2\right)}{\left[\left(1-\varepsilon_1'\beta^2\right)^2 - \left(\varepsilon_2'\beta^2\right)^2\right]}\varepsilon_2'\beta^2,$$
$$\mu_3^* = 1, \quad \xi_{\mathrm{g}}^* = \varepsilon_2, \quad \xi^* = \frac{\left[\left(1-\varepsilon_1'\beta^2\right)\left(\varepsilon_1'-1\right) + \left(\varepsilon_2'\beta\right)^2\right]}{\left[\left(1-\varepsilon_1'\beta^2\right)^2 - \left(\varepsilon_2'\beta^2\right)^2\right]}, \quad \beta = \frac{v_0}{c_0}, \quad \gamma = \frac{1}{\sqrt{1-\beta^2}}, \tag{4}$$

and c_0 is the velocity of light and v_0 is the velocity of MMP. From Eq. (2) we can see that in the stationary frame the MMP is a bi-anisotropic and chiral media.[12,17] Even though, Maxwell equations still lead to the similar non-homogeneous coupled equations for the fields in CWMMP as MMP in circular waveguide:

$$\nabla_{\mathrm{T}}^2 \boldsymbol{E}_z + a^* \boldsymbol{E}_z = b^* \boldsymbol{H}_z + e^* \boldsymbol{J}_z + f^* \rho \boldsymbol{e}_z,$$
$$\nabla_{\mathrm{T}}^2 \boldsymbol{H}_z + c^* \boldsymbol{H}_z = d^* \boldsymbol{E}_z + g^* J_z + h^* \rho, \tag{5}$$

where the coefficients a^*, b^*, c^*, d^*, e^*, f^*, g^* and h^* are given in Appendix.

3. The electromagnetic (EM) fields of the CWMMP

The homogeneous coupled equation (5) can be rewritten as follows:

$$\begin{aligned}\left(\nabla_{\mathrm{T}}^2+p_1^2\right)\left(\nabla_{\mathrm{T}}^2+p_2^2\right)E_z=0,\\ \left(\nabla_{\mathrm{T}}^2+p_1^2\right)\left(\nabla_{\mathrm{T}}^2+p_2^2\right)H_z=0,\end{aligned}\tag{6}$$

where

$$p_{1,2}^2=\frac{(a^*+c^*)\pm\sqrt{(a^*+c^*)^2-4(a^*c^*-b^*d^*)}}{2}.\tag{7}$$

The analytical solution of Eq. (6) can be obtained as

$$\begin{aligned}E_z=&\{[A_m\mathrm{J}_m(p_1r)+B_m\mathrm{N}_m(p_1r)]\\&+[C_m\mathrm{J}_m(p_2r)+D_m\mathrm{N}_m(p_2r)]\}\,\mathrm{e}^{\mathrm{i}m\varphi},\\ H_z=&\{h_1[A_m\mathrm{J}_m(p_1r)+B_m\mathrm{N}_m(p_1r)]\\&+h_2[C_m\mathrm{J}_m(p_2r)+D_m\mathrm{N}_m(p_2r)]\}\,\mathrm{e}^{\mathrm{i}m\varphi},\end{aligned}\tag{8}$$

where $h_1=(a^*-p_1^2)/b^*$, $h_2=(a^*-p_2^2)/b^*$, m is the azimuthal order of mode. And all transverse components of EM fields can be expressed in terms of E_z and H_z (see Appendix). From Eq. (8), we note that the EM fields of the CWMMP are made up of two parts which depend on the eigenvalues p_1 and p_2. Therefore, the eigenvalues affect the characteristics of the two modes. When the eigenvalue is real, the expression of the mode is described by $\mathrm{J}_m(p_{1,2}r)$ and $\mathrm{N}_m(p_{1,2}r)$, and when it is imaginary the expression is described by $\mathrm{I}_m(p_{1,2}r)$ and $\mathrm{K}_m(p_{1,2}r)$. The detailed discussion of the eigenvalues can be seen in Section 4.

Based on Eq. (8) and (A3) shown in Appendix, the dispersion equation can be obtained by using the following boundary conditions:

$$\begin{cases}E_z|_{r=a}=0,\\ E_z|_{r=b}=0,\end{cases}\quad\begin{cases}E_\varphi|_{r=a}=0,\\ E_\varphi|_{r=b}=0.\end{cases}\tag{9}$$

Substituting Eq. (8) into Eq. (9), we can obtain a very complex dispersion equation as shown in Appendix B.

4. Numerical calculation

From Section 3, it is shown that the eigenvalues are very important for the CWMMP, because they determine the expressions of the modes and dispersion characteristics of CWMMP. In this section, based on Eq. (7) we have calculated the eigenvalues by using ω_{p} to normalize the frequency, and c_0 to normalize the velocity.

From Figs. 1–3, it can be found that, in general, below the light line (c line) the eigenvalue p_2 is imaginary and p_1 is real, so the expression of the part corresponds to the case that p_2 is taken as modified Bessel functions $\mathrm{I}_m(p_2r)$ and $\mathrm{K}_m(p_2r)$, the another part corresponds to the case that p_1 is always described by ordinary Bessel function $\mathrm{J}_m(p_1r)$ and $\mathrm{N}_m(p_1r)$. However, there are ω–k_z regions where both eigenvalues are real and imaginary. Figures 1–3 show that the velocity and cyclotron frequency of magnetized plasma (MP) strongly affect the distribution of the eigenvalues, especially in the region below the c-line. Based on the calculations, we can conclude that: (i) when the velocity of the MP is increasing, the ω–k_z regions where both eigenvalues are real and imaginary are increasing correspondingly, and the region where p_2 is imaginary, p_1 is real and shrinking (Figs. 1–3); (ii) it is shown in Figs. 1–3 that because of the relativistic movement of MP, there is a line corresponded to Doppler shift factor ω–$k_zv_0=0$ that splits the area below the c line into two parts, the one is above the line and another is below this line, as shown in the enlarged figure in Figs. 1 and 2. The part above the line ω–$k_zv_0=0$ can also be found in coaxial waveguide filled with stationary magnetized plasma (CWSMP), but the part below that line does not exist in the CWSMP for the Doppler line ω–$k_zv_0=0$ in stationary MP is $\omega=0$ line. It is clearly that because the drift velocity of the MP influences the distribution of eigenvalues of the modes strongly, so the modes in the coaxial and circular[17] waveguides have been changed, especially the slow wave modes, which caused that the dispersion characteristics of CWMMP or MMP in circular waveguide are quite different from the cases of stationary MP.

Figures 4(a) and 4(b) are dispersion characteristics of the CWSMP, from which it can be found that there are three kinds of modes in CWSMP: waveguide modes, cyclotron modes, and plasma modes. And these modes also exist in the CWMMP, however, the relativistic movement of MP greatly influences on the cyclotron modes and plasma modes (Figs. 5 and 6).

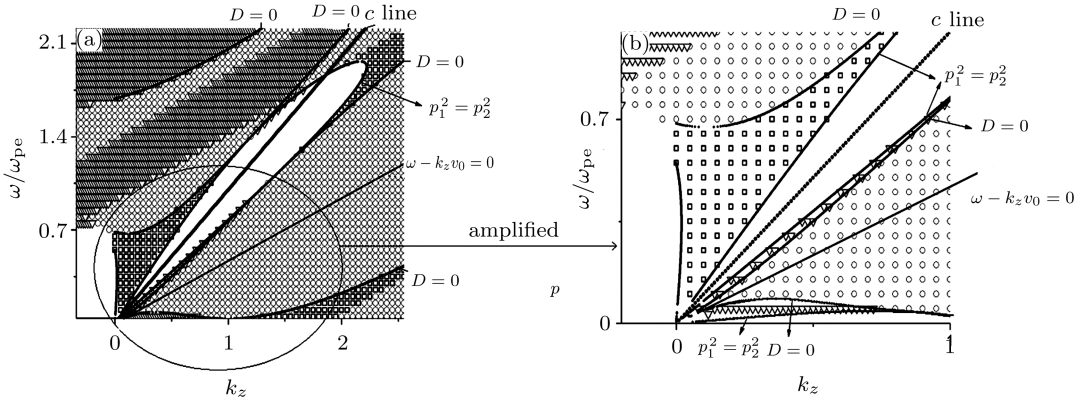


Fig. 1. Eigenvalues of wave propagation along the axis on MP for $v_0 = 0.5c$, $\omega_c = \omega_{pe}$, in the "◯" area $p_1^2 > 0$, $p_2^2 < 0$; in the ∇ area $p_1^{*2} > 0$, $p_2^{*2} > 0$; in the □ area $p_1^{*2} < 0$, $p_2^{*2} < 0$.

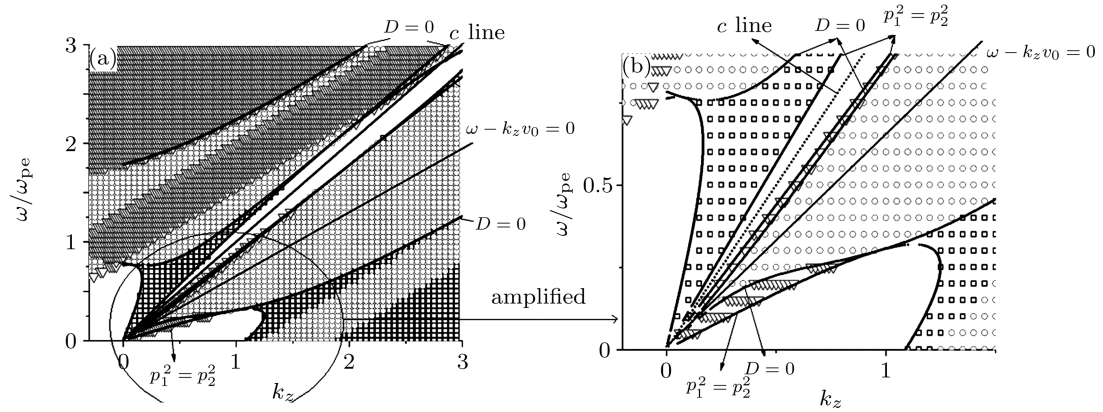


Fig. 2. Eigenvalues of wave propagation along the axis on MP for $v_0 = 0.7c$, $\omega_c = \omega_{pe}$, in the "◯" area $p_1^2 > 0$, $p_2^2 < 0$; in the "∇" area $p_1^2 > 0$, $p_2^2 > 0$; in the □ area $p_1^2 < 0$, $p_2^2 < 0$.

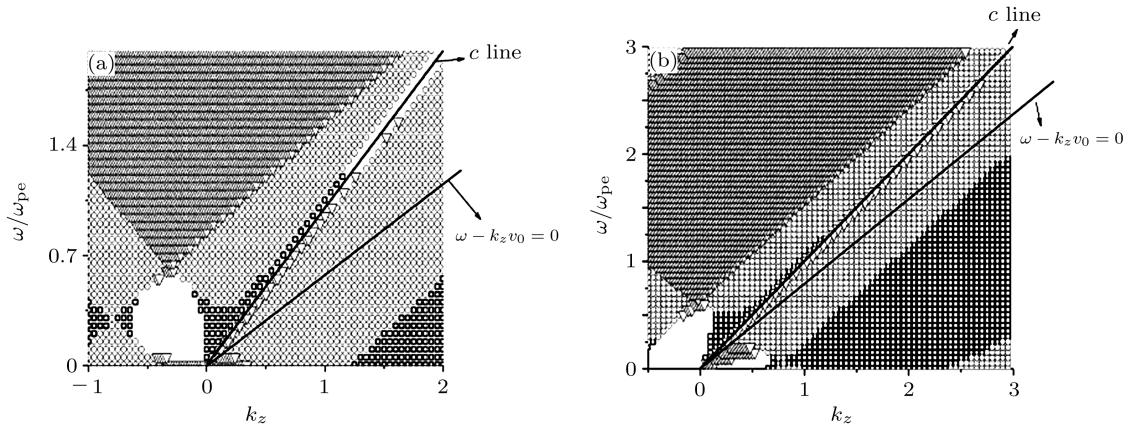


Fig. 3. Eigenvalues of wave propagation along the axis on MP for (a) $v_0 = 0.7c$, $\omega_c = 3\omega_{pe}$, and (b) $v_0 = 0.9c$, $\omega_c = 3\omega_p$. The "◯" area $p_1^2 > 0$, $p_2^2 < 0$; in the "∇" area $p_1^{*2} > 0$, $p_2^{*2} > 0$; in the □ area $p_1^{*2} < 0$, $p_2^{*2} < 0$.

In the CWMMP, there are two groups of plasma modes: 1st group plasma modes and 2nd group plasma modes. It can be found that the 1st group of plasma modes is split by the Doppler line, and the modes above the line can be found in the CWSMP, however, the appearance of the modes below the line is due to the relativistic movement of MP. So in CWMMP, the number of 1st group plasma modes has been much enriched. And there is another 2nd group of plasma modes in the CWMMP which cannot be found in the CWSMP. These modes are very interesting, the starting point of these modes dispersion lines is not from the original point and they are always below the lowest $D = 0$ line (Fig. 5(c)), and they have very low phase velocity. Moreover, the velocity of MMP influences the 2nd group of plasma modes greatly, and when the velocity of MP is very low, this group of modes disappears (Fig. 5(a)).

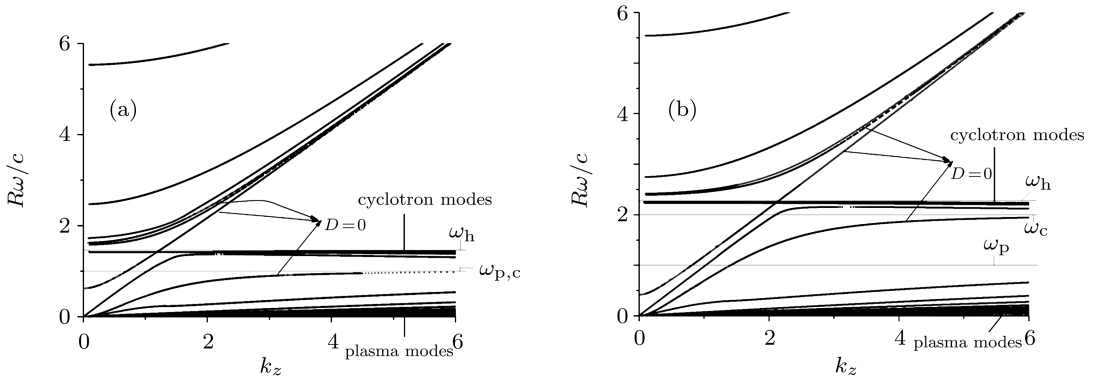


Fig. 4. Dispersion characteristic of CWSMP for $r_{\rm inner} = 0.5$ c/$\omega_{\rm p}$, $r_{\rm outer} = 1.0$ c/$\omega_{\rm p}$, (a) $\omega_{\rm c} = \omega_{\rm pe}$, (b) $\omega_{\rm c} = 2\omega_{\rm pe}$.

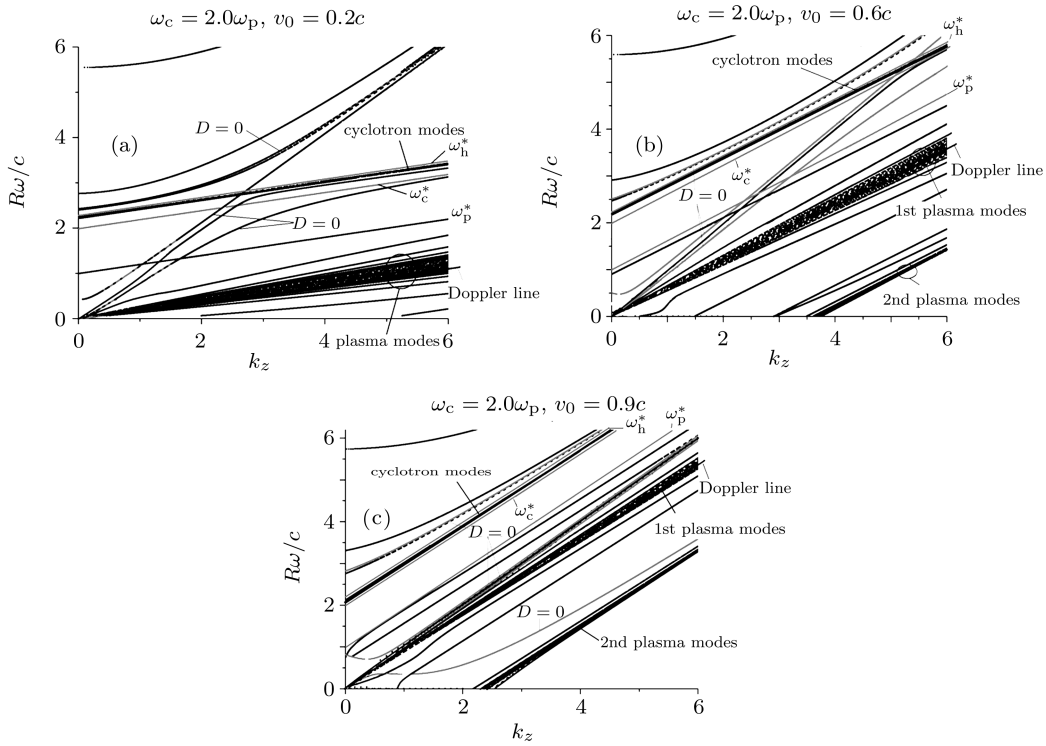


Fig. 5. The influence of the velocity of MP on dispersion characteristic of CWMMP with inner conductor of $r_{\rm inner} = 0.5c/\omega_{\rm p}$ and outer conductor of $r_{\rm outer} = 1.0c/\omega_{\rm p}$, $\omega_{\rm c} = 2\omega_{\rm pe}$ for (a) $v_0 = 0.2$ c, (b) $v_0 = 0.6$ c, and (c) $v_0 = 0.9$ c.

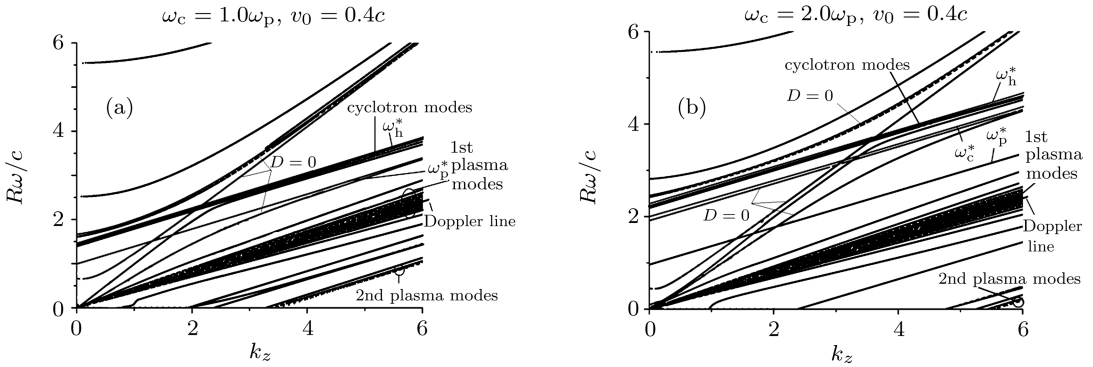


Fig. 6. The influence of the cyclotron frequency of MP on dispersion characteristic of CWMMP with inner conductor of $r_{\rm inner} = 0.5c/\omega_{\rm p}$ and outer conductor of $r_{\rm outer} = 1.0c/\omega_{\rm p}$, $v_0 = 0.4$ c for (a) $\omega_{\rm c} = \omega_{\rm pe}$ and (b) $\omega_{\rm c} = 2\omega_{\rm pe}$.

In the CWMMP, because of Doppler effects, the cutoff frequencies of the three modes are not constants any more, they become functions of k_z and v_z. So in the CWMMP there are no cutoff frequencies for these modes, the cutoff frequencies for the three modes are: $\omega_{\rm p}^* = \omega_{\rm p} + k_z v_z$ for plasma modes; $\omega_{\rm c}^* = \omega_{\rm c} + k_z v_z$ for cyclotron modes; $\omega_{\rm h}^* = \omega_{\rm h} - k_z v_z$ for waveguide modes.

As a key factor, in CWMMP, the velocity of the MMP decides the number of plasma and cyclotron modes (Fig. 5). When the velocity is getting higher, the number of the plasma modes is getting larger and the number of cyclotron modes is decreasing, correspondingly the phase velocity of both kinds of modes is getting higher.

Cyclotron frequency of the MMP affects not only the cyclotron modes but also the plasma modes, especially 2nd group of plasma modes (Fig. 6). The same as CWSMP, in CWMMP it can be found that the cyclotron frequency affects the cyclotron modes (Figs. 4 and 6); with the increase of cyclotron frequency, the number of cyclotron modes is getting larger. However different from CWSMP, in CWMMP cyclotron frequency also strongly affects 2nd group of plasma modes as shown in Fig. 6, when the cyclotron frequency is high enough this group of modes disappears.

Besides the findings mentioned above, it also can be found that the waveguide mode of CWMMP is almost the same as that of CWSMP, so we can conclude that the velocity of MP mainly affects the plasma modes and cyclotron modes, the waveguide modes are not affected by the movement of MP.

Figures 7 and 8 show the influence of the waveguide's size on the dispersion characteristic of CWMMP. It is found that when the radius of outer conductor decreases, the number of plasma modes decreases very fast, especially the 1st group of plasma mode, adversely, the number of cyclotron mode increases. When the radius of inner conductor increases, the number of 1st group of modes decreases sharply and the density of cyclotron modes becomes very little denser.

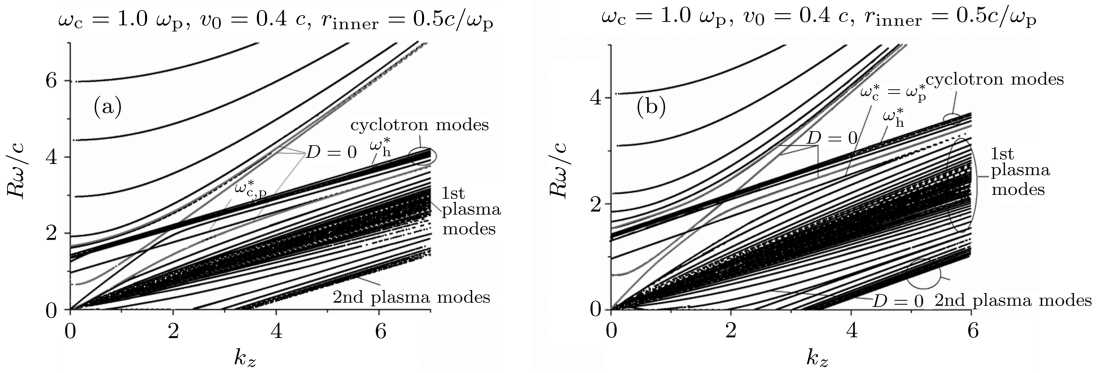


Fig. 7. The influence of the outer radius on dispersion characteristic of CWMMP for (a) $r_{\rm outer} = 2.0c/\omega_{\rm p}$ and (b) $r_{\rm outer} = 3.0c/\omega_{\rm p}$.

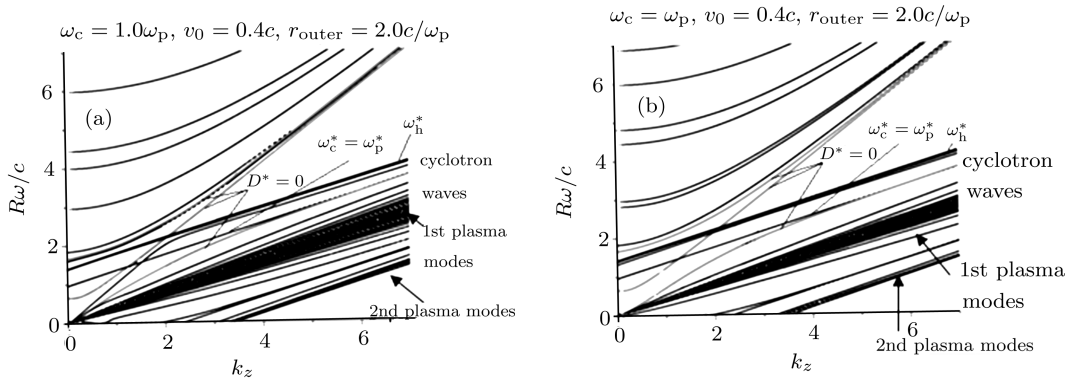


Fig. 8. The influence of the inner radius on dispersion characteristic of CWMMP for (a) $r_{\rm outer} = 1.0c/\omega_{\rm p}$ and (b) $r_{\rm outer} = 1.5c/\omega_{\rm p}$.

So from Figs. 7 and 8, we can find that the plasma modes and cyclotron modes can be controlled by sizing the coaxial waveguide.

5. Conclusion

In this paper, detailed theoretical study on the dispersion characteristic of the CWMMP has been carried out. From the study, some findings about the eigenvalues of the moving MP have been discussed: 1) The EM fields in the CWMMP are made up of two parts with different eigenvalues. And the eigenvalues decide the expressions of the modes. 2) Because of the relativistic movement of MP, the eigenvalues of the fields in CWMMP is quite different from the CWSMP.

Then based on the study of this paper, we can compare the dispersion characteristics between CWMMP with MMP in the circular waveguide.[17] It can be found that there are some commons between them, however there are some important differences as stated below.

(I) For MMP in the circular waveguide, when the plasma drift velocity is high enough, the cyclotron wave modes may disappear. But in CWMMP, although the number of the cyclotron wave modes will decrease with the increase of plasma drift velocity, this group of modes cannot disappear.

(II) In the case of the same plasma drift velocity, the number of plasma modes and cyclotron wave modes in CWMMP is much larger than that for MMP in the circular waveguide, which may cause stronger mode competition in CWMMP.

(III) In CWMMP, we can control the number of plasma modes not only by adjusting the size of outer conductor but also inner conductor.

(IV) For MMP in the circular waveguide, only in the case of high plasma drift velocity the 2nd group of plasma modes will appear. However, in CWMMP even at the relatively low plasma drift velocity, it can also find the 2nd group of plasma modes.

Appendix A

Making use of the Lorentz transformation and the constitutive transformation, the Maxwell equations lead to the coupled wave equations of the CWMMP in the Lab frame.

$$\begin{aligned}\nabla_{\mathrm{T}}^2\boldsymbol{E}_z + a^*\boldsymbol{E}_z &= b^*\boldsymbol{H}_z + e^*\boldsymbol{J}_z + f^*\rho\boldsymbol{e}_z,\\ \nabla_{\mathrm{T}}^2\boldsymbol{H}_z + c^*\boldsymbol{H}_z &= d^*\boldsymbol{E}_z + g^*J_z + h^*\rho,\end{aligned} \tag{A1}$$

$$\begin{aligned}a^* &= k_0^2\mu_1^*\varepsilon_3^* - \frac{\mu_2^*\varepsilon_3^*}{\varepsilon_1^*\mu_1^* - \beta^2\xi_{\mathrm{g}}^{2*}}\left[\mu_2^*\varepsilon_1^*k_0^2 - k_zk_0\beta\xi_{\mathrm{g}}^* - \beta^2\xi_{\mathrm{g}}^*\xi^*k_0^2\right]\\ &+ \frac{(k_0\beta\xi^* + k_z)\varepsilon_3^*}{\varepsilon_1^*\mu_1^* - \beta^2\xi_{\mathrm{g}}^{2*}}\left[-\mu_1^*k_z - \mu_1^*\beta\xi^*k_0 + \beta\xi_{\mathrm{g}}^*\mu_2^*k_0\right],\\ b^* &= \mathrm{i}c_0\mu_0\left\{\xi_{\mathrm{g}}^*\beta\mu_3^*k_0^2 - \frac{k_0\mu_2^*\mu_3^*}{\varepsilon_1^*\mu_1^* - \beta^2\xi_{\mathrm{g}}^{2*}}\left[\varepsilon_1^*k_z + k_0\beta\left(\xi^*\varepsilon_1^* - \xi_{\mathrm{g}}^*\varepsilon_2^*\right)\right]\right.\\ &\left.+ \frac{(k_0\beta\xi^* + k_z)\mu_3^*}{\varepsilon_1^*\mu_1^* - \beta^2\xi_{\mathrm{g}}^{2*}}\left[-\varepsilon_2^*\mu_1^*k_0 + k_0\beta^2\xi^*\xi_{\mathrm{g}}^* + \beta\xi_{\mathrm{g}}^*k_z\right]\right\},\\ c^* &= k_0^2\varepsilon_1^*\mu_3^* - \frac{\varepsilon_2^*\mu_3^*}{\varepsilon_1^*\mu_1^* - \beta^2\xi_{\mathrm{g}}^{2*}}\left[\varepsilon_2^*\mu_1^*k_0^2 - \beta^2\xi_{\mathrm{g}}^*\xi^*k_0^2 - k_zk_0\beta\xi_{\mathrm{g}}^*\right]\\ &- \frac{(k_0\beta\xi^* + k_z)\mu_3^*}{\varepsilon_1^*\mu_1^* - \beta^2\xi_{\mathrm{g}}^{2*}}\left[\varepsilon_1^*k_z + \varepsilon_1^*\beta\xi^*k_0 - \beta\xi_{\mathrm{g}}^*\varepsilon_2^*k_0\right],\\ d^* &= \mathrm{i}c_0\varepsilon_0\left\{-\xi_{\mathrm{g}}^*\beta\varepsilon_3^*k_0^2 + \frac{k_0\varepsilon_2^*\varepsilon_3^*}{\varepsilon_1^*\mu_1^* - \beta^2\xi_{\mathrm{g}}^{2*}}\left[-\mu_1^*k_z - k_0\beta\left(\xi^*\mu_1^* - \xi_{\mathrm{g}}^*\mu_2^*\right)\right]\right.\\ &\left.+ \frac{(k_0\beta\xi^* + k_z)\varepsilon_3^*}{\varepsilon_1^*\mu_1^* - \beta^2\xi_{\mathrm{g}}^{2*}}\left[\mu_2^*\varepsilon_1^*k_0 - k_0\beta^2\xi^*\xi_{\mathrm{g}}^* - \beta\xi_{\mathrm{g}}^*k_z\right]\right\}.\end{aligned}$$

The transverse components of the EM filed can be written as:

$$\begin{aligned}
\boldsymbol{E}_{\mathrm{T}} &= \frac{\left(k_z+k_0\xi\beta\right)^2-k_0^2\varepsilon_2\mu_2}{D^2}\{\omega\mu_0\left\{-\mu_1k_{\mathrm{g}}^2+\mu_2K^2\right\}\boldsymbol{\nabla}_{\mathrm{T}}\boldsymbol{H}_z+\mathrm{i}\left\{k_0\xi_{\mathrm{g}}\beta k_{\mathrm{g}}^2-\left(k_z+k_0\xi\beta\right)K^2\right\}\boldsymbol{\nabla}_{\mathrm{T}}\boldsymbol{E}_z\\
&+\left[\left(k_z+k_0\xi\beta\right)k_{\mathrm{g}}^2-K^2k_0\xi_{\mathrm{g}}\beta\right](\boldsymbol{\nabla}_{\mathrm{T}}\times\boldsymbol{E}_z)+\mathrm{i}\omega\mu_0\left[\mu_2k_{\mathrm{g}}^2-\mu_1K^2\right](\boldsymbol{\nabla}_{\mathrm{T}}\times\boldsymbol{H}_z)\},\\
\boldsymbol{H}_{\mathrm{T}} &= \frac{\left(k_z+k_0\xi\beta\right)^2-k_0^2\varepsilon_2\mu_2}{D^2}\{\omega\varepsilon_0\left(\varepsilon_1k_{\mathrm{g}}^2-\varepsilon_2K^2\right)\boldsymbol{\nabla}_{\mathrm{T}}\boldsymbol{E}_z+\mathrm{i}\left[k_0\xi_{\mathrm{g}}\beta k_{\mathrm{g}}^2-\left(k_z+k_0\xi\beta\right)K^2\right]\boldsymbol{\nabla}_{\mathrm{T}}\boldsymbol{H}_z\\
&-\left[k_0\xi_{\mathrm{g}}\beta K^2-\left(k_z+k_0\xi\beta\right)k_{\mathrm{g}}^2\right](\boldsymbol{\nabla}_{\mathrm{T}}\times\boldsymbol{H}_z)+\mathrm{i}\omega\varepsilon_0\left(\varepsilon_1K^2-\varepsilon_2k_{\mathrm{g}}^2\right)(\boldsymbol{\nabla}_{\mathrm{T}}\times\boldsymbol{E}_z)\}. \qquad \text{(A2)}
\end{aligned}$$

Based on Eq. (A2), we can obtain the complete expression of azimuthally component of EM field:

$$\begin{aligned}
E_\varphi &= \frac{\mathrm{e}^{\mathrm{i}m\varphi}}{D^2}\{\mathrm{i}mA\{h_1\left[A_m\mathrm{J}_m(p_1r)+B_m\mathrm{N}_m(p_1r)\right]+h_2\left[C_m\mathrm{J}_m(p_2r)+D_m\mathrm{N}_m(p_2r)\right]\}-mB\{[A_m\mathrm{J}_m(p_1r)\\
&+B_m\mathrm{N}_m(p_1r)]+[C_m\mathrm{J}_m(p_2r)+D_m\mathrm{N}_m(p_2r)]\}+C\{p_1\left[A_m\mathrm{J}'_m(p_1r)+B_m\mathrm{N}'_m(p_1r)\right]\\
&+p_2\left[C_m\mathrm{J}'_m(p_2r)+D_m\mathrm{N}'_m(p_2r)\right]\}+\mathrm{i}D\{h_1p_1\left[A_m\mathrm{J}'_m(p_1r)+B_m\mathrm{N}'_m(p_1r)\right]\\
&+h_2p_2\left[C_m\mathrm{J}'_m(p_2r)+D_m\mathrm{N}'_m(p_2r)\right]\},\\
H_\varphi &= \frac{\mathrm{e}^{\mathrm{i}m\varphi}}{D^2}\{\mathrm{i}mE\{[A_m\mathrm{J}_m(p_1r)+B_m\mathrm{N}_m(p_1r)]+[C_m\mathrm{J}_m(p_2r)+D_m\mathrm{N}_m(p_2r)]\}-mB\{h_1[A_m\mathrm{J}_m(p_1r)\\
&+B_m\mathrm{N}_m(p_1r)]+h_2\left[C_m\mathrm{J}_m(p_2r)+D_m\mathrm{N}_m(p_2r)\right]\}+C\{h_1p_1\left[A_m\mathrm{J}'_m(p_1r)+B_m\mathrm{N}'_m(p_1r)\right]\\
&+h_2p_2\left[C_m\mathrm{J}'_m(p_2r)+D_m\mathrm{N}'_m(p_2r)\right]\}+\mathrm{i}F\{p_1\left[A_m\mathrm{J}'_m(p_1r)+B_m\mathrm{N}'_m(p_1r)\right]\\
&+p_2\left[C_m\mathrm{J}'_m(p_2r)+D_m\mathrm{N}'_m(p_2r)\right]\}\}. \qquad \text{(A3)}
\end{aligned}$$

Appendix B

Based on the boundary conditions $E_z|_{r=a}=0$, $E_z|_{r=b}=0, E_\varphi|_{r=a}=0$, $E_\varphi|_{r=b}=0$, the dispersion equation can be obtained by solving a matrix:

$$\begin{aligned}
&[m\mathrm{N}_m(bp_2)(-B+\mathrm{i}Ah_2)+\mathrm{N}'_m(bp_2)(C+\mathrm{i}Dh_2)p_2]\\
&\times\{[\mathrm{J}_m(bp_2)\mathrm{N}_m(ap_1)-\mathrm{J}_m(ap_2)\mathrm{N}_m(bp_1)]\left[-m\mathrm{J}_m(ap_1)\left(B-\mathrm{i}Ah_1\right)+p_1\mathrm{J}'_m(ap_1)(C+\mathrm{i}Dh_1)\right]\\
&-[-\mathrm{J}_m(bp_1)\mathrm{J}_m(ap_2)+\mathrm{J}_m(ap_1)\mathrm{J}_m(bp_2)]\left[-m\mathrm{N}_m(ap_1)\left(B-\mathrm{i}Ah_1\right)+p_1\mathrm{N}'_m(ap_1)(C+\mathrm{i}Dh_1)\right]\\
&+[-\mathrm{J}_m(bp_1)\mathrm{N}_m(ap_1)+\mathrm{J}_m(ap_1)\mathrm{N}_m(bp_1)]\left[-m\mathrm{J}_m(ap_2)\left(B-\mathrm{i}Ah_2\right)+p_2\mathrm{J}'_m(ap_2)(C+\mathrm{i}Dh_2)\right]\}\\
&+[m\mathrm{N}_m(bp_1)(-B+\mathrm{i}Ah_1)+\mathrm{N}'_m(bp_1)(C+\mathrm{i}Dh_1)p_1]\\
&\times\{[-\mathrm{J}_m(bp_2)\mathrm{N}_m(ap_2)+\mathrm{J}_m(ap_2)\mathrm{N}_m(bp_2)]\left[-m\mathrm{J}_m(ap_1)\left(B-\mathrm{i}Ah_1\right)+p_1\mathrm{J}'_m(ap_1)(C+\mathrm{i}Dh_1)\right]\\
&-[-\mathrm{J}_m(bp_1)\mathrm{N}_m(ap_2)+\mathrm{J}_m(ap_1)\mathrm{N}_m(bp_2)]\left[-m\mathrm{J}_m(ap_2)\left(B-\mathrm{i}Ah_2\right)+p_2\mathrm{J}'_m(ap_2)(C+\mathrm{i}Dh_2)\right]\\
&+[-\mathrm{J}_m(bp_1)\mathrm{J}_m(ap_2)+\mathrm{J}_m(ap_1)\mathrm{J}_m(bp_2)]\left[-m\mathrm{N}_m(ap_2)\left(B-\mathrm{i}Ah_2\right)+p_2\mathrm{N}'_m(ap_2)(C+\mathrm{i}Dh_2)\right]\}\\
&-[-m\mathrm{J}_m(bp_2)(B-\mathrm{i}Ah_2)+\mathrm{J}'_m(bp_2)(C+\mathrm{i}Dh_2)p_2]\\
&\times\{[-\mathrm{N}_m(bp_2)\mathrm{N}_m(ap_2)+\mathrm{N}_m(ap_1)\mathrm{N}_m(bp_2)]\left[-m\mathrm{J}_m(ap_1)\left(B-\mathrm{i}Ah_1\right)+p_1\mathrm{J}'_m(ap_1)(C+\mathrm{i}Dh_1)\right]\\
&-[-\mathrm{J}_m(bp_1)\mathrm{N}_m(ap_2)+\mathrm{J}_m(ap_1)\mathrm{N}_m(bp_2)]\left[-m\mathrm{N}_m(ap_1)\left(B-\mathrm{i}Ah_1\right)+p_1\mathrm{N}'_m(ap_1)(C+\mathrm{i}Dh_1)\right]\\
&+[-\mathrm{J}_m(bp_1)\mathrm{N}_m(ap_1)+\mathrm{J}_m(ap_1)\mathrm{N}_m(bp_1)]\left[-m\mathrm{N}_m(ap_2)\left(B-\mathrm{i}Ah_2\right)+p_2\mathrm{N}'_m(ap_2)(C+\mathrm{i}Dh_2)\right]\}\\
&-[m\mathrm{J}_m(bp_1)(-B+\mathrm{i}Ah_1)+\mathrm{J}'_m(bp_1)(C+\mathrm{i}Dh_1)p_1]\\
&\times\{[-\mathrm{J}_m(bp_2)\mathrm{N}_m(ap_2)+\mathrm{J}_m(ap_2)\mathrm{N}_m(bp_2)]\left[-m\mathrm{N}_m(ap_1)\left(B-\mathrm{i}Ah_1\right)+p_1\mathrm{N}'_m(ap_1)(C+\mathrm{i}Dh_1)\right]\\
&-[-\mathrm{N}_m(bp_1)\mathrm{N}_m(ap_2)+\mathrm{N}_m(ap_1)\mathrm{N}_m(bp_2)]\left[-m\mathrm{J}_m(ap_2)\left(B-\mathrm{i}Ah_2\right)+p_2\mathrm{J}'_m(ap_2)(C+\mathrm{i}Dh_2)\right]\\
&+[\mathrm{J}_m(bp_2)\mathrm{N}_m(ap_1)-\mathrm{J}_m(ap_2)\mathrm{N}_m(bp_1)]\left[-m\mathrm{N}_m(ap_2)\left(B-\mathrm{i}Ah_2\right)+p_2\mathrm{N}'_m(ap_2)(C+\mathrm{i}Dh_2)\right]\}\\
&=0,
\end{aligned}$$

where

$$A = \omega\mu_0\left\{-\mu_1^* k_{\rm g}^2 + \mu_2^* K^2\right\},\quad B = \left\{k_0\xi_{\rm g}^*\beta k_{\rm g}^2 - (k_z + k_0\xi^*\beta)\,K^2\right\},\quad C = \left[(k_z + k_0\xi^*\beta)\,k_{\rm g}^2 - K^2 k_0\xi_{\rm g}^*\beta\right],$$
$$D = \omega\mu_0\left[\mu_2^* k_{\rm g}^2 - \mu_1^* K^2\right],\quad E = \omega\varepsilon_0\left(\varepsilon_1^* k_{\rm g}^2 - \varepsilon_2^* K^2\right),\quad F = \omega\varepsilon_0\left(\varepsilon_1^* K^2 - \varepsilon_2^* k_{\rm g}^2\right),$$
$$K^2 = k_0^2\left(\varepsilon_1^*\mu_1^* + \mu_2^*\varepsilon_2^*\right) - \left(\xi_{\rm g}^*\beta k_0\right)^2 - (k_z + k_0\xi^*\beta)^2,\quad k_{\rm g}^2 = k_0^2\left(\varepsilon_1^*\mu_2^* + \mu_1^*\varepsilon_2^*\right) - 2\,(k_z + k_0\xi^*\beta)\,k_0\xi_{\rm g}^*\beta.$$

And when $p_{1,2}$ is imaginary the corresponding Bessel functions become I_m and K_m.

References

[1] Chu K R 2004 *Rev. Mod. Phys.* **76** 489

[2] Granatstein V L and Alexeff I 1987 *High-Power Microwave Sources* (Boston: Artech House)

[3] Rosebury F 1965 *Handbook of Electron Tube and Vacuum Techniques* (MA: Addison Wesley)

[4] Carmel Y L, Antonsen W R, Rodgers T M, Levush J, Tate B, Destler J and Granatstein V 1992 *Phys. Fluids* B **4** 2286

[5] Miller S M, Antonsen T M and Levush B 1998 *IEEE Trans. Plasma Sci.* **26** 680

[6] Goebel D M, Ponti E S, Eisenhart R L and Lemke R W 1999 *Phys. Plasmas* **6** 2225

[7] Hoffman J R, Muggli P and Liou R 2001 *J. Appl. Phys.* **90** 1115

[8] Gao H and Liu S G 2000 *Chin. Phys.* **9** 274

[9] Li W and Gong M L 2004 *Chin. Phys.* **13** 54

[10] McKinstrie C J 1988 *Phys. Fluids* **31** 1273

[11] Sawthney R and Minami K 1993 *IEEE Trans. Plasma Sci.* **21** 609

[12] Liu S G, Wei Y Y, Yuan X S and Yan Y 2007 *J. Appl. Phys.* **101** 053309

[13] Yasumoto K 1983 *Radio Science* **18** 207

[14] Kong J A and Cheng D K 1981 *IEEE Trans. Microwave Theory Tech. MTT* **16** 99

[15] Allen H B 1981 *Phys. Fluids* **24** 1387

[16] Nakagawa K 1990 *J. Appl. Phys.* **67** 6125

[17] Liu S G, Yan Y, Mao J and Manos D M 2002 *Phys. Rev.* E **65** 036411